A Parameter-free Radial Distortion Correction of Wide Angle Lenses using Distorted Vanishing Points

Wonsik Kim, Young Ki Baik, and Kyoung Mu Lee

School of Electrical Engineering and Computer Science, Seoul National University,
`ultra16@snu.ac.kr, hyunxx00@snu.ac.kr, kyoungmu@snu.ac.kr`

Abstract In this paper, we proposed a new stratified method for correcting the radial distortion of a strong wide-angle lens using a single image. The key idea is to use a 3D concave calibration rig with three planar patterns aligned orthogonally with each other. The parallelism of the line patterns, orthogonality and concavity of the rig enable us to deal with the distortion of the entire image that is obtained even by a strong wide field of view (FOV) lens such as fish-eye lens. First, by identifying vanishing points in the distorted image with curved lines, we can estimate the center of distortion. And then, ideal vanishing points and straight lines are restored, so that the undistorted image is recovered. Since our method is parameter-free and does not rely on any particular radial distortion model, it can be applied to various types of lenses. Experimental results demonstrate the effectiveness and robustness of the proposed method.

1 Introduction

1.1 Radial distortion

The exponential growth of computational storage and processing power make it possible for the computer vision to deal with real applications rather than theoretical problems. For real vision applications, we have to solve practical problems related imaging optics, illumination, noise, etc. The lens distortion is one of them.

Unlike the ideal pinhole lens of a perspective camera model, in practice, a real lens usually exhibits some nonlinear distortion in mapping to an image plane. So, the lens distortion is a fundamental problem of all forms of camera especially for the camera with a wide FOV like a fish-eye camera. Slama [1] divided the lens distortion into radial and decentering terms. In general, the radial term is considered as a more significant part of lens distortion [2], and the decentering term is commonly obtained by recursive method using the pre-estimated radial distortion parameters as initial values.

The radial distortion is a 2D to 2D mapping that is non-linear and radially symmetric. Also, it is assumed that the radial distortion changes nothing but the distance from the center of distortion to an image point in monotonically increasing fashion. Therefore, the clue for solving the radial distortion is to figure out the position of the center of distortion and the parameters of the distortion model.

1.2 Previous works

There have been lots of methods to solve the radial distortion problem. Heikkila [5] classified them into two categories: the coupling method and the decoupling method. The coupling method is to find out a solution with getting together projective and distortion parameters at the same time in the framework of camera calibration [1]. This method is efficient when the amount of distortion is small. In case of the image with severe distortion, however, this method does not work well despite of large number of iterations, due to its sensitivity to the initial value and tendency to be in local minima. In contrast, the decoupling method is to determine the parameters by separating projective and distortion terms independently [2]. This approach is intuitive and non-iterative, while it depends on the accuracy of the pre-computed parameters. Most of decoupling methods use pre-defined model for radial distortion by using various image features such as point, line, sphere from some artificial rig or natural scene [7, 10, 6, 4]. These methods can be validated only when the chosen model is similar to the real lens distortion. Recently, parameter-free methods have been proposed [9, 12], in which the principal point and the corresponding samples between distorted and undistorted image are estimated. And more recently, Kannala et. al. tried to combine both the coupling and decoupling methods to enhance the overall accuracy [11].

For the correction of radial distortion, some scene geometry and its properties should be incorporated. For this purpose, commonly a calibration rig (a plane or cubic) with specific pattern on it or natural scene has been used. However, the experimental results of using natural scene tend to be sensitive to the number and distribution of the sample features which are used in estimating the parameters. And, although using a planar calibration pattern is an effective method to estimate the corresponding sample pairs in the distorted and undistorted image, it can not cover the whole FOV especially when the distortion is severe. So, in order to solve this problem, we need to use an extremely large planar pattern, which is practically infeasible.

1.3 Contribution of this paper

In this paper, we propose a new parameter-free stratified method for correcting radial distortion by estimating the vanishing points and slopes of projected lines that are parallel in 3D space. A special calibration rig is designed for this purpose, so that the entire image can cover the calibration patterns, and three orthogonal vanishing points are observed in the image. Our method is parameter free and independent on the lens distortion model. The main contributions of this paper can be summarized as follows:
• Design of a special calibration rig that can cover the whole image area of wide-angle lens.
• Development of a new center of distortion estimation method using the distorted vanishing points.
• Development of distortion correction method using vanishing points and parallel line information only, so that finding exact correspondences between samples in the distorted and the undistorted images is possible without any information of the external parameters of a camera.

2 Calibration rig and patterns for distortion correction

Figure 1(a) shows the specially designed calibration rig for radial distortion correction. The rig is composed of three planar patterns aligned concavely and orthogonally. In contrast to commonly used planar patterns, the rig can cover the whole image even under the presence of severe radial distortion of a wide-angle lens as shown in Figure 1(b). So it helps us to figure out every distortion occurred in the whole image area. Moreover, by using orthogonality of three planes, we can estimate the principal points and corrected grid points deterministically without any external camera parameters. Detailed description will be presented in next Section.
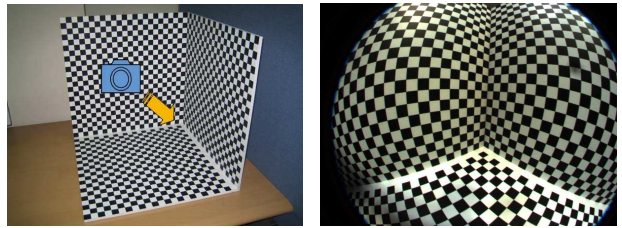

Fig. 1: (a) Calibration rig for lens distortion correction. (b) A distorted image of the rig pattern by a wide angle lens.

3 Estimation of the center of distortion(COD)

In this section, we propose a method to estimate the COD directly by locating the distorted vanishing points. As Hartley and Kang [9] and Stein [13], argued, in this work, we assume that the COD could be displaced from the principal point.

In fact, we can not apply the conventional concept of vanishing points to a distorted image directly since the parallel lines in 3D space are transformed to the curved lines on the distorted image. Thus, we need to examine the properties of the projected vanishing points on the distorted image, and the relation to the COD.

The formation of vanishing points in a distorted image is well depicted in Figure 2. On the ideal perspective image plane, a vanishing point is defined by the intersection of extended straight lines which are parallel to each other in 3D space as shown in Figure 2(a). If radial distortion is occurred on the image, then the straight line becomes a curved one as depicted in Figure 2(b). We can approximate and extend this curve using an arc of a circle [7] or any higher order curve model. Then, we can find a pair of intersection points of those extended curves, and those points are the distorted vanishing points. With these vanishing points, the COD can be identified by the following theorem.
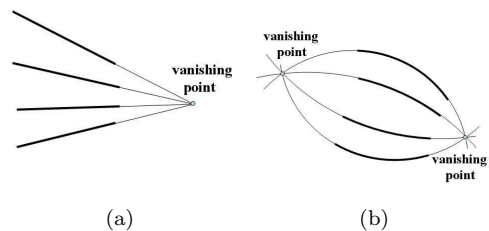

Fig. 2: (a) Formation of a vanishing point on undistorted image. (b) Transformed vanishing points and lines on distorted image
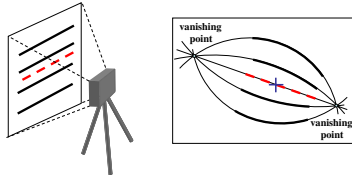
Fig. 3: Illustrated figure shows that a pair of vanishing points and the center of distortion (blue cross) are collinear.

Theorem 1. The center of distortion is the intersection point of straight lines connecting each pair of distorted vanishing points in the distorted image.

Proof. Consider a set of coplanar parallel lines in 3D space as shown in figure 3(a) (black lines). These lines will form two vanishing points in the distorted image as in figure 3(b). There exists a line in this set, of which projected line passes the center of distortion (red dashed lines in figure 3). Since the distortion occurs in radial direction, this line becomes a straight line passing through the two vanishing points in the distorted image. This means that the center of distortion and the two vanishing points are collinear. And, consequently the center of distortion is the intersection of straight lines that connects pairs of vanishing points in the distorted image. □

4   Rebuilding undistorted image

The goal of this section is to find exact correspondences of every sample (feature) point between distorted and corrected image. We set sample points to be the intersection points between lines of the pattern. Now let us explain how to find the corrected sample points in the undistorted image.

4.1   Finding undistorted vanishing point

Every sample line in the undistorted image will pass through one of the undistorted vanishing points. This fact will help us to find every corrected line. In Section 3, we have found six distorted vanishing points of three set of parallel lines which are orthogonal to each other. We now show how we can recover the real three undistorted vanishing points by using those distorted ones.

We exploit the geometric interpretation of the relationship between three vanishing points and the principal point in an undistorted image. When three vanishing points are formed by three mutually
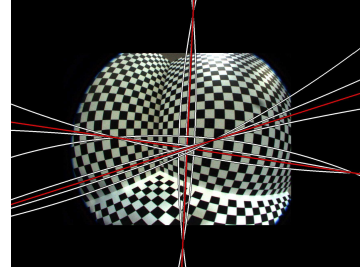

Fig. 4: Finding the distortion center by using six distorted vanishing points. Each group of curves makes two distorted vanishing points a line connecting them. The distortion center is the crossing point of the three lines connecting the vanishing points.

orthogonal sets of parallel lines in the 3D, the principal point is the orthocenter of the triangle with the vanishing points as vertices [8]. Thus, if we know the positions of three vanishing points, we can easily find the position of the principal point. We note that the reverse is also true, and this can be used to determine the undistorted vanishing points. In our case, we have the principal point and three lines that the distorted vanishing points lie on. Since we are considering radial distortion, the undistorted vanishing point must lie on the line connecting two corresponding distorted vanishing points passing through the principal point. So, the undistorted vanishing points can be found by drawing arbitrary triangle with the three lines as perpendicular lines of its each side. The scale of the triangle, surely, has not yet been determined exactly. This scale problem will be discussed in Section 4.4.

4.2   Finding the slopes of undistorted lines

In the following, we present how to recover the slopes of every sample line in the undistorted image. In Figure 5, line $\mathbf{l}$ and $\mathbf{l}'$ denote a straight
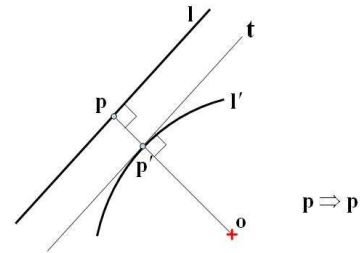

Fig. 5: $\mathbf{l}$ is undistorted line and $\mathbf{l}'$ is the corresponding distorted line. The tangent line $\mathbf{t}$ at $\mathbf{p}'$ of $\mathbf{l}'$ is parallel to $\mathbf{l}$, so the slopes of them are same.

line and the corresponding curved one in the undistorted and distorted images, respectively.

Assume that $\mathbf{p}$ is the closest point on the undistorted line $\mathbf{l}$ to the principal point $\mathbf{o}$. Then, line $\mathbf{l}$ and line $\mathbf{po}$ is orthogonal. The point $\mathbf{p}'$ that is transformed one of $\mathbf{p}$, lies on the line $\mathbf{po}$ and is still the closest point of the distorted line $\mathbf{l}'$ to the principal point, since a radial distortion function only changes the distance to the distortion center not the orientation. Note that since the tangential line $\mathbf{t}$ of $\mathbf{l}'$ at $\mathbf{p}'$ is orthogonal to the line $\mathbf{p}'\mathbf{o}$, and the lines $\mathbf{po}$ and $\mathbf{p}'\mathbf{o}$ are identical, line $\mathbf{l}$ and $\mathbf{t}$ are parallel to each other. Therefore, the slope of $\mathbf{t}$ at $\mathbf{p}'$ is the same as the slope of original straight line $\mathbf{l}$. Now, by using this information, we can reconstruct the undistorted sample lines which are parallel in 3D space by simply translating the obtained tangent lines so that they pass through the corresponding undistorted vanishing point found in Section 4.1.

4.3   Correction of the slope error

In practice, due to some measurement noise and numerical error, the slopes we calculated might not be exact. So, in this section we propose a method to correct the calculated slope values by using a relevant geometric constraint.

Let us consider the general relationship between the imaged lines of coplanar equally spaced parallel lines in 3D space by a pine-hole camera. The set of coplanar equally spaced parallel lines can be written by

$$\mathbf{l}'_n = (a, b, n)^T = (a, b, 0)^T + n(0, 0, 1)^T, \quad (1)$$

where $\mathbf{l}'_1, \mathbf{l}'_2, \ldots, \mathbf{l}'_n, \ldots$ are 2D homogeneous coordinates of parallel lines, and $(0, 0, 1)^T$ is the line at infinity on the scene plane [8]. When these parallel lines are captured by a perspective camera, they will be transformed by a homography $\mathbf{H}$ as follows.

$$\mathbf{l}_n = \mathbf{H}^{-T}\mathbf{l}'_n = \mathbf{l}_0 + n\mathbf{l}_\infty \quad (2)$$

where $\mathbf{l}_0 = (l_{01}, l_{02}, l_{03})^T$ is the image of $(a, b, 0)^T$ and $\mathbf{l}_\infty = (l_{\infty 1}, l_{\infty 2}, l_{\infty 3})^T$ is the image of $(0, 0, 1)^T$, the vanishing line. Then,

$$\mathbf{l}_n = (l_{01} + nl_{\infty 1}, l_{02} + nl_{\infty 2}, l_{03} + nl_{\infty 3}) \quad (3)$$

Let θ_n be the angle between $\mathbf{l}_\infty$ and $\mathbf{l}_n$. Then we have the following relationship.

$$(\tan \theta_n)^{-1} = \frac{l_{\infty 1}l_{01} + l_{\infty 2}l_{02} + n(l_{\infty 1} + l_{\infty 2})}{l_{\infty 1}l_{02} - l_{\infty 2}l_{01}}$$
$$= cn + d \quad (4)$$

where

$$c = \frac{l_{\infty 1} + l_{\infty 2}}{l_{\infty 1}l_{02} - l_{\infty 2}l_{01}} \quad \text{and} \quad d = \frac{l_{\infty 1}l_{01} + l_{\infty 2}l_{02}}{l_{\infty 1}l_{02} - l_{\infty 2}l_{01}}$$
$$(5)$$

We can use (6) as a constraint for the projected lines of equi-spaced parallel coplanar lines in 3D space, and utilize it for correcting the estimated slope values of the reconstructed lines.

Let $a_n, n = 1, 2, \ldots, N$ be the series of estimated angles between each estimated undistorted line and the corresponding vanishing line, then we can find the parameter c^* and d^* that minimize the following least square error.

$$E = \sum_n \left(\frac{1}{\tan a_n} - (c^*n + d^*) \right)^2 \quad (6)$$

Once obtained the optimal parameters, we can correct the line angles so that satisfy the constraint in (6) by

$$\hat{a}_n = \arctan\left(\frac{1}{c^*n + d^*} \right), \quad n = 1, 2, \ldots, N \quad (7)$$

4.4   Finding the scaling factor

Up to now, we have found the principal point, undistorted vanishing points, and corrected straight lines. So we can establish the correspondences between the distorted sample (grid) points and undistorted ones. However, note that we have determined the positions of vanishing points up to scale in Section 4.1. So, the scaling factor is still unknown, and the correspondences are also up to scale.

In order to determine the scale factor, we use the fact that the distortion is very small and negligible in the vicinity of the principal point [3]. So, by finding and comparing the areas of two corresponding squares that includes the principal points in the distorted and recovered undistorted image, respectively, we can determine the scale factor that makes two area same. Now, the exact correspondences between the sample points in the distorted and undistorted images can be established.

5   Applying various distortion models

The final step is to apply various user-defined distortion models to the estimated correspondences. Note that this procedure is totally independent on the previous steps. The parameters of the distortion

functions can be determined by minimizing the error between points obtained from previous step and those from applying distortion functions. By comparing errors on each distortion function, we can choose the most appropriate distortion model.

6 Experimental Results

6.1 Synthetic image test

We have tested the proposed algorithm with synthetic images. At first, we have generated synthetic ideal perspective images of grid points on three orthogonal patterns using arbitrary camera matrix P. Then, we distorted the ideal images by the FOV distortion model [6] with a distortion parameter value ω=0.003. Next, we disturbed the sample points by random noise with standard deviations of $\sigma = 0.0$, 0.1, 0.2 and 0.5 pixels in both x- and y-coordinates. We then have corrected it by using the proposed method.

σ	$E_x \pm S_x$	$E_y \pm S_y$
0.0	0.00±0.00	0.00±0.00
0.1	0.11±0.33	0.06±0.25
0.2	0.43±0.65	0.26±0.51
0.5	2.74±1.65	1.82±1.35

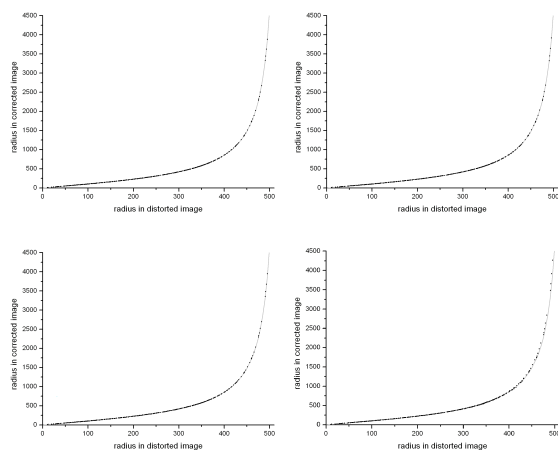Table 1: Accuracy of the estimated distortion center (in pixels)

Fig. 6: Plots of the estimated distortion function (in pixels)according to the noise variation. Dots represent the estimated correspondences between distorted and corrected images, and the solid line represents the ground truth distortion function. (a) σ = 0.0, (b) σ = 0.1, (c) σ = 0.2, and (d) σ = 0.5 pixels.
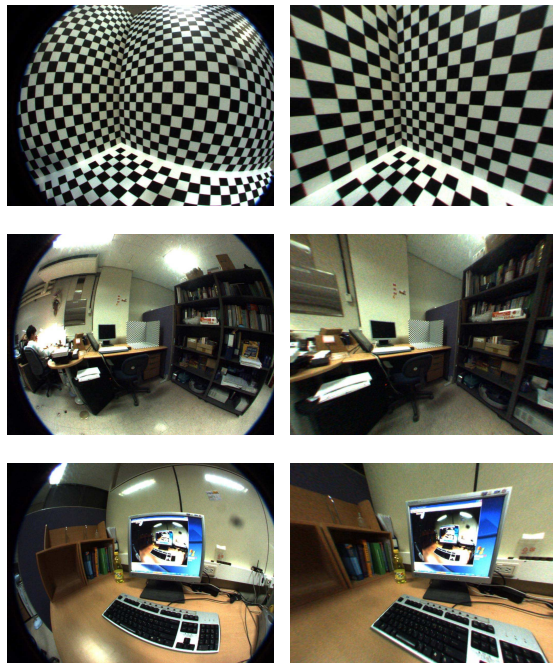

Fig. 7: Experimental results with real images. Left column show the input distorted images and the right column displays the corresponding corrected images.

The results have been evaluated by two ways. Firstly, the accuracy of the estimated principal point according to the noise variation was investigated. Experiments were performed 50 times per each case. The true principal point was at (562, 434). Mean errors (E_x, E_y) of the principal point and standard deviations (S_x, S_y) were calculated and summarized in Table 1. Secondly, we investigated how well the estimated corresponding samples in the distorted and corrected images fit to the true distortion function that we used to distort the ideal image. Figure 6 show the resultant plots according to the variation of noise in which dots are the estimated correspondences and the solid line represents the ground truth distortion function. These experimental results surely demonstrates the robustness and immunity of the proposed algorithm against noise.

6.2 Real image test

We have also tested our algorithm on real images. The fish-eye lens used in the experiment was FUJINON FE185C046HA-1 which had 185° field of view. The resolution of image was 1024 x 768. At first, we took an image of the calibration rig with three planar patterns by a camera with the lens. as shown in Figure 7(a). The size of each planar pattern was

480 mm x 480 mm and that of a square grid was 20 mm x 20 mm. Figure 7(b) illustrates the corrected image by our method. After finding correspondences between sample points and comparing several model errors using them, we have chosen the FOV model [6] as the most appropriate radial distortion function for the lens. So, once the distortion model and its parameters were determined, we applied it for the correction of several natural images taken by the same camera. The results are shown in Figure 7 (c)-(f), in which the left column represents the distorted images and the right column displays the corresponding corrected images by our method. We note from these results that the proposed algorithm works quite satisfactory that all the straight lines are recovered almost perfectly in the corrected images.

7 Conclusion

We proposed a new algorithm for correcting radial distortion of wide angle lenses. The basic idea is to utilize the parallelism of the line patterns on three orthogonal planes and its projective properties on the ideal and distorted image planes. First it determines the distortion center using the distorted vanishing points directly, and then reconstructs the ideal vanishing points as well as the undistorted straight lines using some geometric interpretations. Finally the correspondences between the distorted and undistorted sample points are easily established, which can be used for estimating the distortion function. In order to treat the whole distortion area in a view even for a very strong wide-angle lens, we designed a special calibration rig that consists of three mutually orthogonal planes aligned concavely. And parallel lines and grids patterns are printed on each plane. The proposed approach is parameter free and independent to any particular distortion model, so it is applicable to large range of cameras. Experimental results on synthetic and real images demonstrated that the proposed algorithm was quite accurate and robust to noise and the degree of distortion. In this work, we did not consider the decentering factor and the possible displacement between the distortion center and the principal point. So, our future work will be to address these problems.

References

[1] C. C. Slama: Manual of photogrammetry, American Society of Photogrammetry, 1980.

[2] R. Y. Tsai: A versatile camera calibration technique for high-accuracy 3D machine vision metrology using off-the-shelf TV cameras and lenses, IEEE J.Robotics and Automation, vol.3, No.4, pp323-344, 2004.

[3] S. Shah and J. K. Aggarwal: A simple calibration procedure for fish-eye (high distortion) lens camera, Proceedings of IEEE International Conference on Robotics and Automation, vol.4, pp3422-2427, 1994.

[4] B. Prescott and G. F. McLean: Line-based correction of radial lens distortion, Graphical Models and Image Processing, vol.59, No.1, pp39-47, 1997.

[5] J. Heikkila: Geometric camera calibration using circular control points, IEEE Trans. Pattern Analysis and Machine Intelligence, vol.22, No.19, pp1066-1077, 2000.

[6] F. Devernay and O. Faugeras: Straight lines have to be straight, Machine Vision and Applications, vol.13, pp14-24, 2001.

[7] C. Brauer-Burchardt and K. Voss: A new algorithm to correct fish-eye and strong wide-angle-lens- distortion from single images, International Conference of Image Processing(ICIP), vol.1, pp225-228, 2001.

[8] R. I. Hartley and A. Zisserman: Multiple view geometry in computer vision, 2nd Ed, Cambridge:CUP, 2003.

[9] R. Hartley and S. B. Kang: Parameter-free Radial Distortion Correction with Centre of Distortion Estimation, Proceedings of the Tenth IEEE International Conference on Computer Vision, pp.1834-1841, 2005.

[10] D. Claus and A. W. Fitzgibbon: A rational function lens distortion model for general cameras, Conference on Computer Vision and Pattern Recognition(CVPR 2005), vol.1, pp213-219, 2005.

[11] J. Kannala and S. S. Brandt: A Generic Camera Model and Calibration Method for Conventional, Wide-Angle, and Fish-Eye Lenses, IEEE Trans.Pattern Analysis and Machine Intelligence, vol.28, No.8, 2006.

[12] H. Li and R. Hartley: Plane-Based Calibration and Auto-calibration of a Fish-Eye Camera, Asian Conference on Computer Vision (ACCV), pp21-30, 2006.

[13] G. P. Stein: Accurate internal camera calibration using rotation, with analysis of sources of error, International Conference on Computer Vision (ICCV), pp 230–236, 1995.